The Journal of CPRI,
Vol. 10, No. 2, June 2014 pp. 287-294

Space-vector Based Equal Switching Strategy for Three-level Open-end Winding Induction Motor Drive

Srinivasan Pradabane*, Narasimharaju B L*, Srikanth N V* and Deshpande R A**

This paper proposes a new space-vector based pulse width modulation strategy for a three-level open-end winding induction motor drive. The proposed method incorporates both the clamping and switching duties of the inverters within every 60^o span of the rotation of the reference space vector.The proposed scheme neither requires sector identification nor lookup tables for the generation of the gating pulses. The switching pattern adopted in the present work ensures equal clamping duty and switching duty for both the inverters which are electrically isolated from each other to suppress the zero sequence currents. The switching strategy ensures the usage of all the clamping states thus making the drive system possible for maximum utilization of the switching resources. The proposed strategy is simulated using MATLAB/Simulink and experimentally validated using dSPACE.

Keywords: *Open-end winding, Space vector modulation, Switching loss, Conduction loss, Inverter.*

1.0 INTRODUCTION

Multilevel converters can produce stepped voltage waveform with low harmonic distortion [1]. The stress that occur on the power semiconductor switches are also reduced as the voltage levels are lesser in the multilevel inversion topologies. This increased the research interest among the scholars around the globe. Several topologies have been put forth in the past three decades. Few multilevel topologies are Neutral-point-clamped inverters [2], series connected H-bridge inverters [3] and dual inverter fed open-end winding induction motor drive [4]. Few PWM schemes for openend winding induction motor was proposed [8]-[11].

This paper proposes a new space-vector based PWM schemes for an open-end winding induction motor drive, which ensures both the clamping and the switching duties for both the inverters within 60^o of the rotation of the space vector. The open-end winding induction motor drive offers rich switching redundancy which has been exploited and effectively utilized to clamp one inverter while to switch the other inverter during a particular span of space vector. This ensures that all the active vectors are used as clamping states for one inverter during clamping duty. The proposed strategy requires neither the sector-identification nor the lookup tables.

2.0 OPEN-END WINDING INDUCTION MOTOR DRIVE

The open-end winding induction motor drive is obtained by opening the neutral-point of the star connected stator windings of the conventional three phase induction motor and feeding the motor from either end using inverters Figure 1.

* NationalInstitute of Technology, Warangal-506 004, E-mail : spradabane2000@yahoo.co.in
**Central Power Research Institute, Bangalore-560080. Mobile: +91 9449056349, E-mail: rad@cpri.in

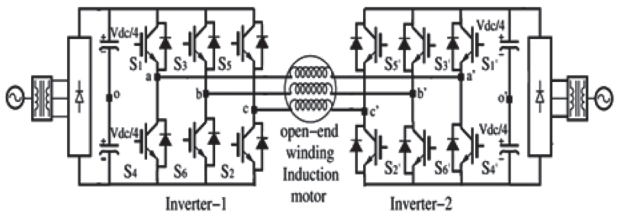

FIG. 1 DUAL INVERTER FED OPEN-END WINDING INDUCTION MOTOR DRIVE CONFIGURATION WITH ISOLATION

If it is fed from a single source, it causes zero sequence currents to flow, which is deleterious to the switching devices and the motor itself. To suppress the zero sequence components in the motor phases, each inverter is operated with an isolated DC power supply. When isolated DC power supplies are used for individual inverters, the zero sequence current cannot flow as it is denied a path. Consequently, the zero sequence voltage appears across the points 'O' and 'OO'.

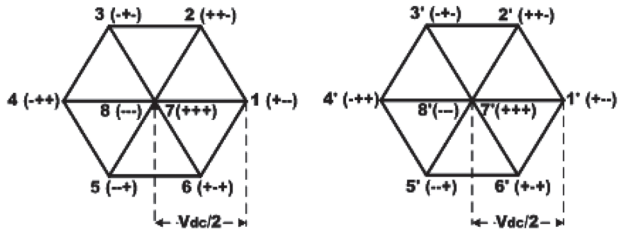

(A) VOLTAGE VECTORS FOR INV-1 AND INV-2

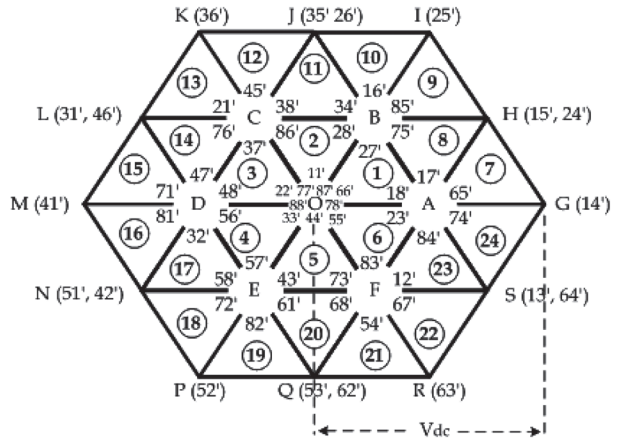

(B) SPACE VECTOR LOCATIONS FOR A 3-LEVELDUAL INVERTER SCHEME.

FIG. 2 THREE-LEVEL HEXAGONAL STRUCTURE SHOWING SPACE VECTOR LOCATIONS OBTAINED FROM INDIVIDUAL INVERTERS

It can also be seen that in dual-inverter scheme, the DC-link voltage of individual inverters is equal to $V_{dc}/2$, whereas the DC-link voltage of an equivalent single inverter drive is equal to V_{dc}. It was shown that three-level inversion can be obtained with the use of two two-level inverters feeding the open-end winding induction motor drive [2].

TABLE 1

STATES OF INDIVIDUAL INVERTERS

State of Inv-1	Switches turned ON	State of Inv-2	Switches turned ON
1 (+ □ □)	S6, S1, S2	1' (+ □ □)	S6', S1', S2'
2 (++ □)	S1, S2, S3	2' (++ □)	S1', S2', S3'
3 (□ + □)	S2, S3, S4	3' (□ + □)	S2', S3', S4'
4 (□ ++)	S3, S4, S5	4' (□ ++)	S3', S4', S5'
5 (□ □ +)	S4, S5, S6	5' (□ □ +)	S4', S5', S6'
6 (+ □ +)	S5, S6, S1	6' (+ □ +)	S5', S6', S1'
7 (+++)	S1, S3, S5	7' (+++)	S1', S3', S5'
8 (□ □ □)	S2, S4, S6	8' (□ □ □)	S2', S4', S6'

Each of the two level inverters can attain eight switching states independent of each other as in Table 1; therefore, a total of 64 switching combinations are possible with the dual-inverter scheme. For example, the switching combination 24' means that inverter-1 would attain state '2' while inverter-2 attains state '4'.

TABLE 2

POLE VOLTAGES AND MOTOR PHASE VOLTAGE

Pole Voltage of Inv-1	Pole Voltage of Inv-2	Motor Phase Voltage
Vdc/2	Vdc/2	0
Vdc/2	-Vdc/2	Vdc
-Vdc/2	-Vdc/2	0
-Vdc/2	Vdc/2	-Vdc

The dual inverter scheme can produce 64 switching combinations spread over the 19 space vector locations, and forms 24 sectors Figure 2. It can be observed that switching locations are similar to Neutral Point Clamped (NPC) three-level inverter; however, with the dual-inverter scheme, redundant switching combinations are available to realize a particular location. The three-level space vector structure consists of a

core hexagon 'ABCDEF' centered around 'O' and six other sub-hexagons namely OBHGSF, OCJIHA, ODLKJB, OENMLC, OFQPND and OASRQE centered around the points A, B, C, D, E and F, respectively.

Any leg of the two inverter scan in dependentl yatta in levels '0'or 'Vdc/2'. The voltage a cross a particular phase winding can be obtained by

$$V_{AA}' = V_{A0} - V_A'_0 \quad ....(1)$$

$$V_{BB}' = V_{B0} - V_B'_0 \quad ....(2)$$

$$V_{CC}' = V_{C0} - V_C'_0 \quad ....(3)$$

The phase winding scan attainone of the levels, '0', '-Vdc/2', and '+Vdc/2' Table 2. The effect of the voltages in the three windings can bere presented by a voltage space vector Vsr as defined by

$$V_{sr} = V_{AA}' + V_{BB}' . e^{(j2pi/3)} + V_{CC} . e^{(-j2pi/3)} \quad ....(4)$$

From eqn.(4) the voltage space vector locations for different switching com binations are shown in Figure 3. This voltage evector can be equivalently represented as the sum of the voltage space vectors generated by the two two-level inverters. If Vs1and Vs2 are the voltage space vectors generated by inverter-1 and inverter-2, respectively, there sultant voltage space vectoris

$$V_{sr} = V_{S1} + V_{S2} \quad ....(5)$$

In this drive, the two inverters are operated with a common DC-link voltage. Inverter-1 and inverter-2 are operated witha DC-link voltage of Vdc/2. Thus, the sum of the DC-link voltages is equal to Vdc, which is the DC-link voltage of an equivalent conventional two-level inverter drive.

3.0 ALTERNATE SUB-HEXAGONAL CENTRE PWM SWITCHING SCHEME

The principle of alternate sub-hexagonal centre (alternate-SHC) PWM switching strategy is depicted Figure 4. In this PWM strategy, the reference voltage space vector 'OV', with its tip 'V' situated in sector '7' is resolved into two components, namely, 'OA' and 'AT'.Vector 'OA' is realized by clamping one inverter and the component 'AV' is synthesized by switching the other inverter.The clamping vector 'OA' remains unaltered throughout the 60° span, wherein the tip of the reference vector 'OV' lies in the quadrangle OSGH.For the situation depicted Figure 3, the clamping vector 'OA' can be obtained by clamping the inverter-1 to state-1 (+ - -) and switching inverter-2 around it.

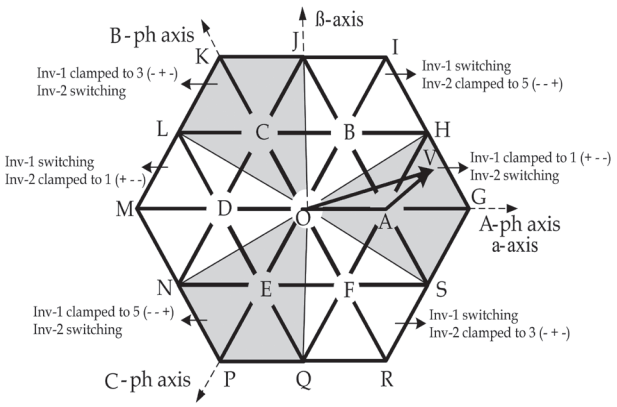

FIG. 3 PRINCIPLE OF ALTERNATE-SHC PWM STRATEGY

TABLE 3

INVERTER ROLES FOR REALIZING THE REFERENCE SPACE VECTOR

NSHC	Inverter-1	Inverter-2
A	Clamped to 1 (+ - -)	Switched
B	Switched	Clamped to 5 (- - +)
C	Clamped to 3 (- + -)	Switched
D	Switched	Clamped to 1 (+ - -)
E	Clamped to 5 (- - +)	Switched
F	Switched	Clamped to 3 (- + -)

In alternate-SHC switching scheme, if the SHC is 'A', 'C' or 'E', inverter-1 is used as the clamping inverter while inverter-2 will be used as the switching inverter as in Table 3. At the other SHCs namely, 'B', 'D' and 'F', inverter-2 is used as the clamping inverter while inverter-1 as the switching inverter. Thus the inverters change their roles as clamping and switching inverters

depending on the SHC for every 60˚ of the cycle Figure 4. The Nearest Sub-Hexagonal Centre (NSHC) is found based only on the magnitudes of the three instantaneous phase reference voltages. It is important to note that the clamping state of the clamping inverter and also the switching times of the switching inverter are dependent entirely on the instantaneous three-phase reference voltages.

4.0 PROPOSED SPACE VECTOR BASED PWM SWITCHING SCHEME

In this proposed PWM strategy, the reference voltage space vector 'OV', with its tip 'V' situated in sector '9' is resolved into two components, namely, 'OB' and 'BV'. Since the Space vector is in the NSHC-B, Vector 'OB' is realized by clamping inverter-1 to state 2 (+ + -) and the component 'BV' is synthesized by switching inverter-2. The clamping vector 'OB' remains unaltered throughout the 30˚ span (i.e. from 30^o to 60^o). Again as the reference space vector moves and crosses 60^o, inverter-2 is clamped to state 5 (- - +), while inverter-1 is switched around it. Thus with the space vector's location dictates the clamping and switching modes of the inverters with a change of alpha by 30° as in Table 4. For every 30^o both the inverters alternate their clamping and switching duties, irrespective of the NSHC which is illustrated in Figure 4.

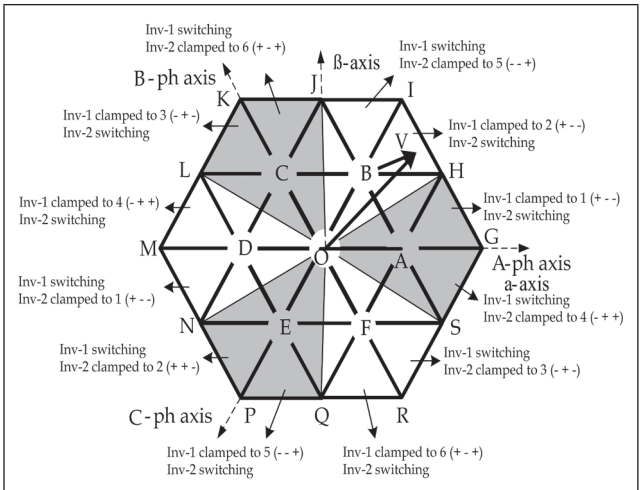

FIG. 4 PRINCIPLE OF PROPOSED-SHC PWM STRATEGY

In this work, the space-vector-based PWM scheme presented for the conventional two-level inverter [3] is extended for the dual-inverter scheme. The switching timings for the switching inverter are calculated, which depend only on the instantaneous phase reference voltages. The clamping states of the clamping inverter (be it inverter-1 or inverter-2) also depend on the instantaneous phase reference voltages.

TABLE 4

INVERTER ROLES FOR REALIZING THE REFERENCE SPACE VECTOR IN THE PROPOSED PWM SCHEME

Alpha	NSHC	Inverter-1	Inverter-2
0 to 30^o	A	Clamped to 1 (+ - -)	Switched
30^o to 60^o	B	Clamped to 2 (+ + -)	Switched
60^o to 90^o		Switched	Clamped to 5 (- - +)
90^o to 120^o	C	Switched	Clamped to 6 (+ - +)
120^o to 150^o		Clamped to 3 (- + -)	Switched
150^o to 180^o	D	Clamped to 4 (- + +)	Switched
180^o to 210^o		Switched	Clamped to 1 (+ - -)
210^o to 240^o	E	Switched	Clamped to 2 (+ + -)
240^o to 270^o		Clamped to 5 (- - +)	Switched
270^o to 300^o	F	Clamped to 6 (+ - +)	Switched
300^o to 330^o		Switched	Clamped to 3 (- + -)
330^o to 360^o	A	Switched	Clamped to 4 (- + +)

5.0 RESULTS AND DISCUSSION

The proposed PWM scheme is implemented using 4-pole, 5-hp three phase open-end winding induction motor drive. Gating pulses are given to the inverters using dSPACE. The control signals are capable of starting the induction motor smoothly. The simulation results are shown in Figure 5 for modulation index of 0.4. In this mode the two-level inversion is obtained. Figure

5(a) shows the pole voltage of inverter-1 and Figure 5(b) shows the pole voltage of inverter-2. The difference of pole voltage is shown in Figure 5(c). Since both the inverters are operated with isolated power supplies, zero sequence currents are denied a path. The zero sequence voltage is measured either across the positive rail DC-link or at the negative rail of the DC-link, which is shown in Figure 5(d). After deducting the zero sequence voltage from the difference of the motor pole voltages, the motor phase voltage is obtained which is depicted in Figure 5(e). Motor phase voltage is illustrated in Figure 5(f). Simulated motor phase voltages for a linear modulation index of 0.8 as in Figure 6(a) and for over modulation region in Figure 6(b).

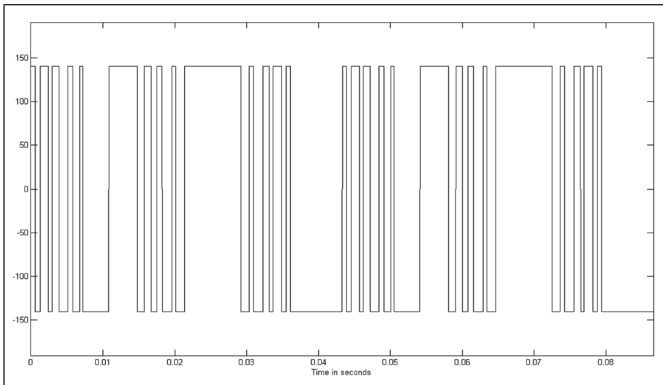

(A) POLE VOLTAGE FOR INVERTER-1

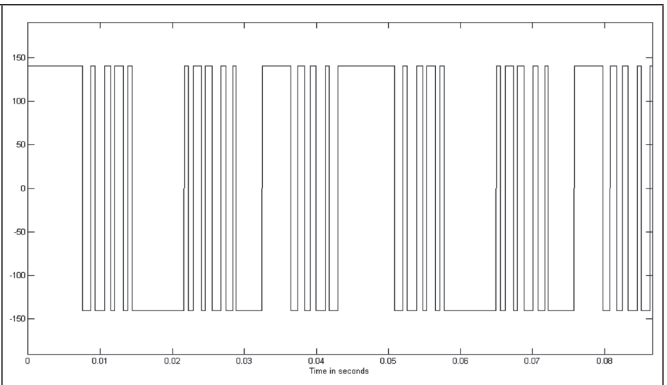

(B) POLE VOLTAGE FOR INVERTER-2

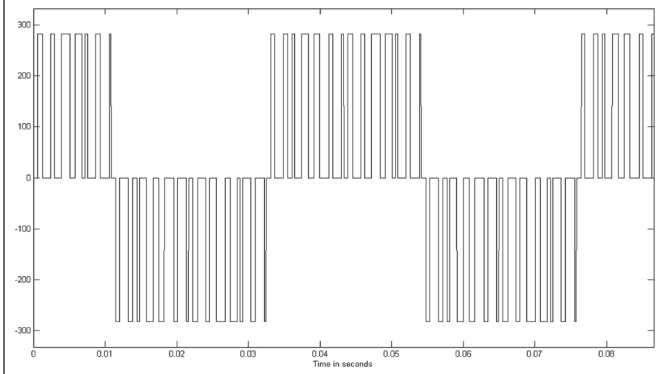

(C) DIFFERENCE OF POLE VOLTAGES

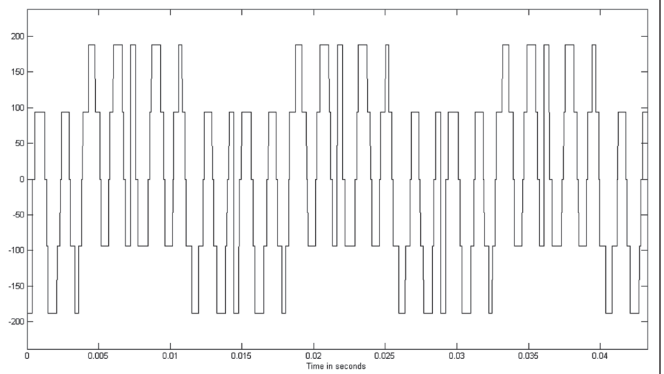

(D) ZERO SEQUENCE VOLTAGE

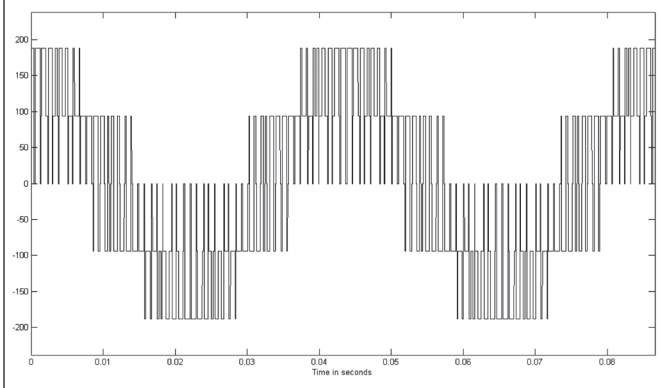

(E) MOTOR PHASE VOLTAGE

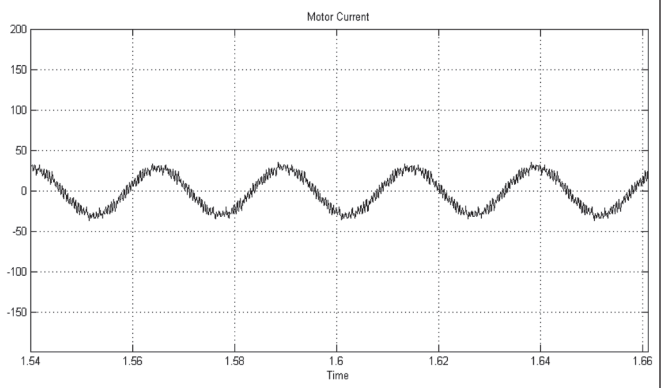

(F) MOTOR CURRENT

FIG. 5 SIMULATED RESULTS FOR THE PROPOSED-SHC PWM SCHEME

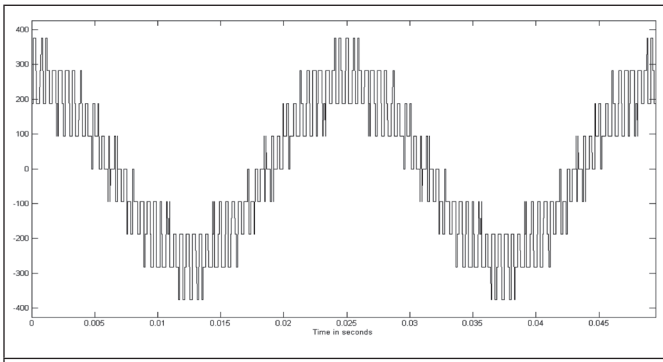

(A) MOTOR PHASE VOLTAGE FOR MA=0.8

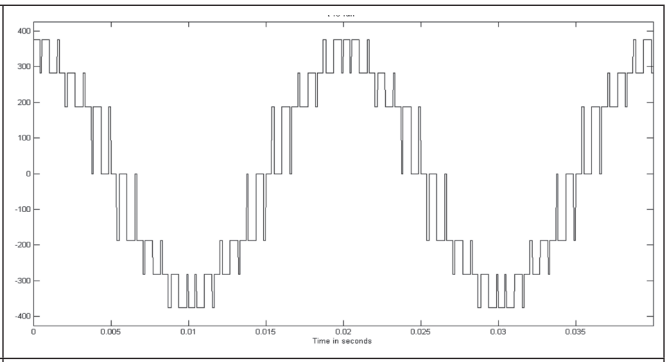

(B) MOTOR PHASE VOLTAGE FOR MA=1

FIG. 6 SIMULATED RESULTS FOR THE PROPOSED-SHC PWM SCHEME

Figure 7 shows the experimentally obtained results for the proposed PWM scheme for a modulation index of m_a=0.4. In Figure 7(a), the top and middle traces show the gating signals obtained using dSPACE. The bottom trace shows the difference of the gating signals derived as a function of pole voltages. Figure 7(b) depicts the zero sequence voltage which is measured across negative rail of the DC-link. Figure 7(c) shows the motor phase voltage (top trace) and currents (bottom trace).

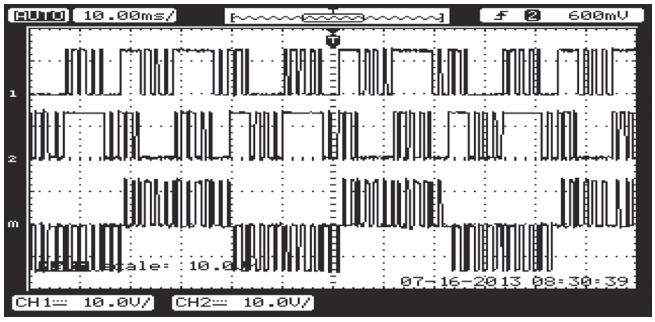

(A) GATING PULSES DERIVED AS A FUNCTION OF POLE VOLTAGES FOR: INVERTER-1 (TOP TRACE); INVERTER-2 (MIDDLE TRACE) ANDDIFFERENCE OF POLE VOLTAGES (BOTTOM TRACE)

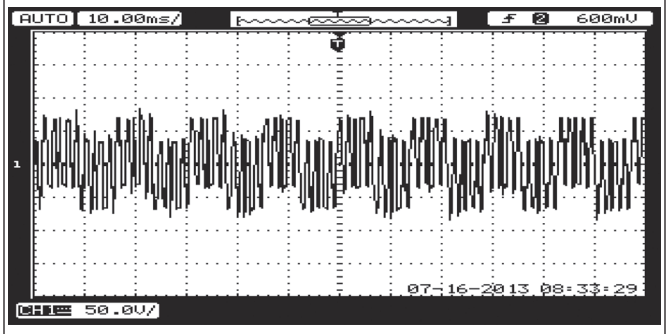

(B) ZERO SEQUENCE VOLTAGE

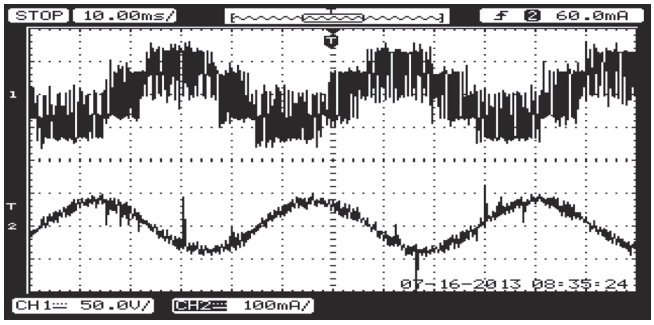

(C) MOTOR PHASE VOLTAGE (TOP TRACE) AND MOTOR CURRENT (BOTTOM TRACE)

FIG. 7 EXPERIMENTALLY OBTAINED RESULTS FOR MA=0.4

Figure 8 shows the experimentally obtained results for the proposed PWM scheme for a modulation index of m_a=0.8.

In Figure 8(a), the top and middle traces show the gating signals obtained using dSPACE. The bottom trace shows the difference of the gating signals derived as a function of pole voltages. Figure 8(b) depicts the zero sequence voltage which is measured across negative rail of the DC-link. Figure 8(c) shows the motor phase voltage (top trace) andcurrents (bottom trace).

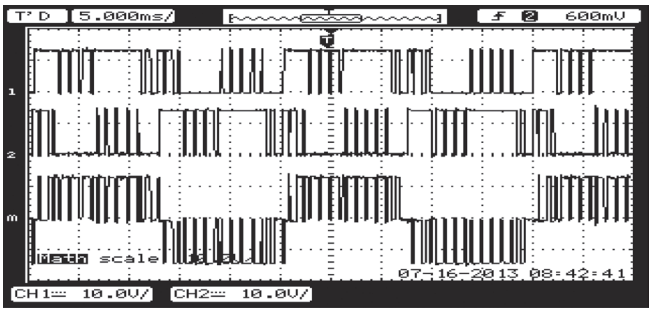

(A) GATING PULSES DERIVED AS A FUNCTION OF POLE VOLTAGES FOR: INVERTER-1 (TOP TRACE); INVERTER-2 (MIDDLE TRACE) ANDDIFFERENCE OF POLE VOLTAGES (BOTTOM TRACE)

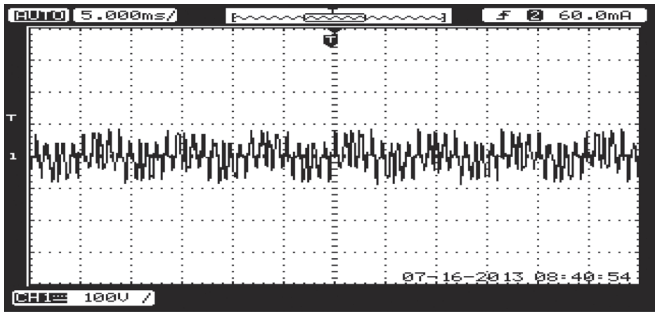

(B) ZERO SEQUENCE VOLTAGE

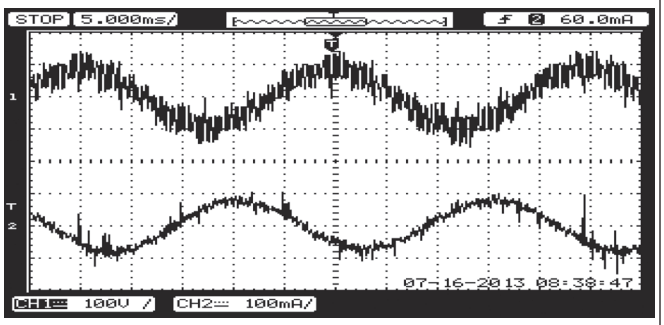

(C) MOTOR PHASE VOLTAGE (TOP TRACE) AND MOTOR CURRENT (BOTTOM TRACE)

FIG. 8 EXPERIMENTALLY OBTAINED RESULTS FOR MA=0.8

Figure 9 shows the experimentally obtained results for the proposed PWM scheme for over modulation region. In Figure 9(a), the top and middle traces show the gating signals obtained using dSPACE. The bottom trace shows the difference of the gating signals derived as a function of pole voltages. Figure 9(b) depicts the zero sequence voltage which is measured across negative rail of the DC-link. Figure 9(c) shows the motor phase voltage (top trace) and currents (bottom trace).

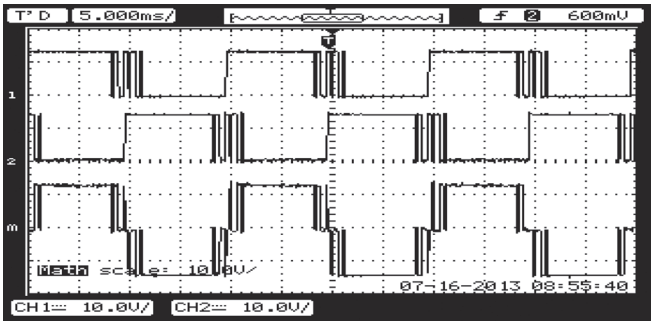

(A) GATING PULSES DERIVED AS A FUNCTION OF POLE VOLTAGES FOR: INVERTER-1 (TOP TRACE); INVERTER-2 (MIDDLE TRACE) ANDDIFFERENCE OF POLE VOLTAGES (BOTTOM TRACE)

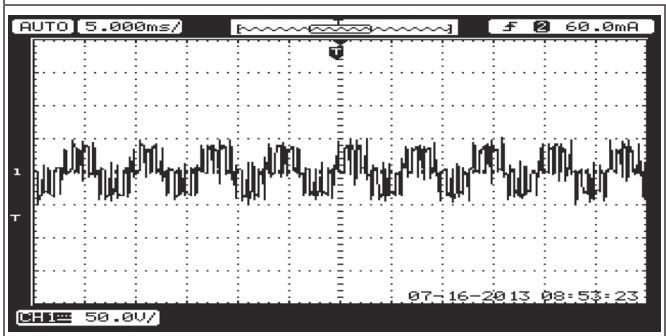

(B) ZERO SEQUENCE VOLTAGE

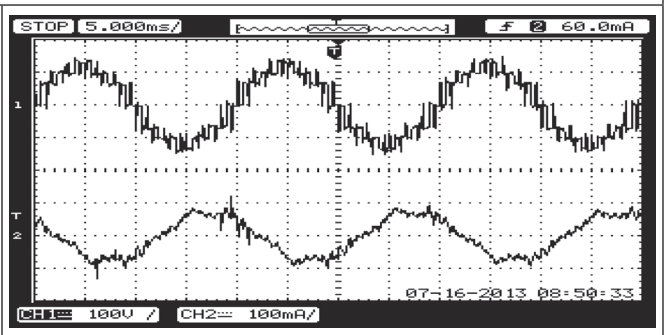

(C) MOTOR PHASE VOLTAGE (TOP TRACE) AND MOTOR CURRENT (BOTTOM TRACE)

FIG. 9 EXPERIMENTALLY OBTAINED RESULTS FOR MA=1 (OVER MODULATION)

6.0 CONCLUSION

In this paper, a space vector-based PWM scheme is proposed. The proposed scheme is simulated using MATLAB/Simulink and validated experimentally using dSPACE. This scheme allows one inverter to switch for one complete cycle while the other inverter is clamped and vice-versa every 30^o. This PWM scheme uses all the active clamping states for both the inverters unlike only few states are used in the scheme reported earlier [4-7]. The switching frequency of each inverter is half of the motor phase switching frequency. This scheme requires two isolated power supplies so that the zero sequence currents are denied a path which is deleterious for the power semiconductor devices. Relocation of the effective time within a sampling time period ensures that all the space vector locations are used. These types of inverter-fed drive systems can be used in electric powered automotives as the size of the inverter is halved.

REFERENCES

[1] A. Nabae, L. Takahashi, and H. Agaki. 1981, A new neutral point-clamped PWM Inverter, IEEE Trans. Ind. Appl., Vol. IA-17, pp518-523.

[2] H. Stemmler, P. Guggenbach, Configurations of high power voltage source inverter drives, EPE 1993, Brighton, U.K., pp.7-12.

[3] Kim. J. S., Sul. S. K., Anovel voltage modulation technique of the space vector PWM, IPEC 1995, Conf. Proc., pp.742–747.

[4] Somasekhar. V. T., Srinivas. S., and Gopa kumar. K, A space vector based PWM switching scheme for the reduction of common-mode voltages for a dual inverter fed open-end winding induction motor drive, IEEE-PESC-2005, Recife, Brazil, 2005, pp. 816–821.

[5] Srinivasan Pradabane, B.V. Reddy, PWM switching strategy for the elimination of common mode voltage of a two-level inverter drive with an open-end winding induction motor configuration, Conf. Proc. PEDES 2010 Power India.

[6] V. T. Somasekhar, S. Srinivas, 2008, Space-vector-based PWM switching strategies for a three-level dual-inverter-fed open-end winding induction motor drive and their comparative evaluation, IET Electr. Power Appl., 2, (1), pp. 19–31.

[7] V. T. Somasekhar, Srirama Srinivas, and Kommuru Kranti Kumar, Effect of Zero-Vector Placement in a Dual-Inverter Fed Open-End Winding Induction Motor Drive With Alternate Sub-Hexagonal Center PWM Switching Scheme, IEEE Transactions on Power Electronics, Vol. 23, no. 3.

[8] E. G. Shivakumar, K. Gopakumar, S. K. Sinha, A. Pittet, and V. T. Rangathan, Space vector PWM control of dual inverter fed open-end winding induction motor drive, IEEE APEC 2001, pp. 399–405.

[9] Chunduri Sreeharsha, Annurag Das, Srinivasan Pradabane, Study of sinusoidal and space vector pulse width modulation techniques for a cascaded three-level inverter, IJRET, vol. 2 n. 9, pp. 365-370.

[10] Srinivasan Pradabane, N. V. Srikanth, B.L. Narasimharaju, "A New Alternate Fixed-bias Inverter SVPWM scheme for Open-end Winding Induction Motor Drive", International Review of Electrical Engineering, Vol. 9, No. 1, pp. 1 - 6, Feb 2014.

[11] Srinivasan Pradabane, N.V. Srikanth, B.L. Narasimharaju, "Investigation of Device Temperature on Power Electronics Switches used in Open-end Winding Induction Motor Drive for Alternate Fixed-bias Inverter Scheme", International Review of Electrical Engineering, Vol. 9, No. 1, pp. 36 - 41, Feb 2014.